



# A Novel Design of a Quadratic Koch Fractal Nano Antenna for THz Application

Ammar Nadal Shareef<sup>1</sup>, Amer Basim Shaalan<sup>2</sup>, Hayder Salah Naeem<sup>1</sup>, Mustafa Albairi<sup>3,\*</sup>

<sup>1</sup>College of Basic Education, Al-Muthanna University, Samawah, Iraq

<sup>2</sup>College Of Science, Al-Karkh University, Baghdad, Iraq

<sup>3</sup>Çankaya University, Department of Civil Engineering, Yukarıyurtçu Mah.Mimar Sinan Cad. No: 4, Etimesgut, 06790 Ankara, Turkey

Emails: [ammarnadhal@mu.edu.iq](mailto:ammarnadhal@mu.edu.iq); [hs985@mu.edu.iq](mailto:hs985@mu.edu.iq); [ame72r@gmail.com](mailto:ame72r@gmail.com); [c2290007@student.cankaya.edu.tr](mailto:c2290007@student.cankaya.edu.tr)

## Abstract

The study, called "A Novel Design of a Quadratic Koch Fractal Nanoantenna," aims to create and study a brand-new microstrip nanoantenna that works in the THz range, specifically between 100 and 130 THz, and can handle a wide range of optical communication frequencies. We examine two unique geometries, specifically the quadratic Koch fractal patch (QKF) and the complementary quadratic Koch fractal patch (CQKF), utilizing two different dielectric materials as substrates. We employ silicon (Si) dielectric material because of its high dielectric constant (11.9), while we use the silicon dioxide (SiO<sub>2</sub>) dielectric material because of its dielectric constant (4). The feeding method employed to stimulate these nanoantennas has been waveguide feed at a frequency of 50 Ω. We have employed a software simulator, available for purchase as CST STUDIO SUITE, to achieve the established objectives for assessing the performance of each proposed nanoantenna.

**Keywords:** Quadratic Koch Fractal; Nanoantenna; Terahertz Applications; Microstrip antenna

## 1. Introduction

A Nano-antenna, often referred to as an optical antenna, resembles a typical antenna in that it interacts with electromagnetic waves; however, it specifically function. The electromagnetic spectrum includes the infrared (IR) frequency band. The size of the antenna should match the operating wavelength, and to attain resonance at infrared frequencies, antennas should shrink to nanoscale dimensions. A nano-antenna is a metallic structure at the nanometer scale that enhances the interaction of optical radiation with matter [1–3]. In 1959, Richard Feynman proposed the concept of reconfiguring materials at the nanoscale level [4]. A few decades later, researchers became aware of nanotechnology thanks to these inspired scientific concepts. Advancements in nanotechnology have garnered significant interest from researchers in optical antennas, owing to their diverse applications, including solar cells, spectroscopy, microscopy, biomedical, and energy harvesting [5–9]. However, researchers have not extensively examined conventional antenna difficulties such as impedance matching, gain, and far-field characteristics, which are critical for wireless communication antennas. In 2010, Nader Engheta proposed the optical antenna as an alternative to optical waveguides for optical wireless broadcasting links in inter and intra-chip optical communication [10]. As compared to significant advancements within a microwave transmitter technology, research in optical antennas remains very nascent. In addition to the challenges of creating nanoscale structures, the techniques for designing microwave circuits are still in their infancy. Therefore, a straightforward miniaturization traditional approaches to antenna theory and design are impractical. Consequently, the emerging theory for Nano scaled antennas must consider phenomena that are unique at optical wavelengths [11,12]. Mandelbrot originally described fractals as a method for categorizing structures with non-integer dimensions [13]. Fractal shapes are useful in antenna design due to their ability to reduce size, multiband frequency response, wideband properties, frequency independence (uniform performance across a wide range of frequencies), and a

decrease in array antennas' mutual coupling [14–16]. Different researchers have looked into how fractal geometries can be used in RF/microwave antennas and found that some shapes are better for making antennas smaller [16–18], while others focus on making designs that use multiple bands [19–21]. Only a limited number of publications have addressed nanofractal antennas, unlike microwave antennas, to leverage the advantages of fractal geometry [22]. Utilizing fractal concepts in optical antennas makes them even smaller and may greatly reduce cooperation in upcoming high-density plasmonic networks, such as nano-antenna solar cell applications, where effective nano-antenna solar panels are made up of a huge number of them [23]. This is in addition to giving them multiband or wideband properties and reliable performance across the operational frequency range.

## 2. Proposed Method

CST Studio is responsible for rapid and accurate three-dimensional electromagnetic modeling in high-frequency scenarios. This module encompasses several solutions that function in both the time and frequency domains. The finite integration approach (FIT) underpins the time-domain (transient) solver employed in computational tomography (CT). Figure 1 illustrates the sequence of the simulation process that transpires in CST.

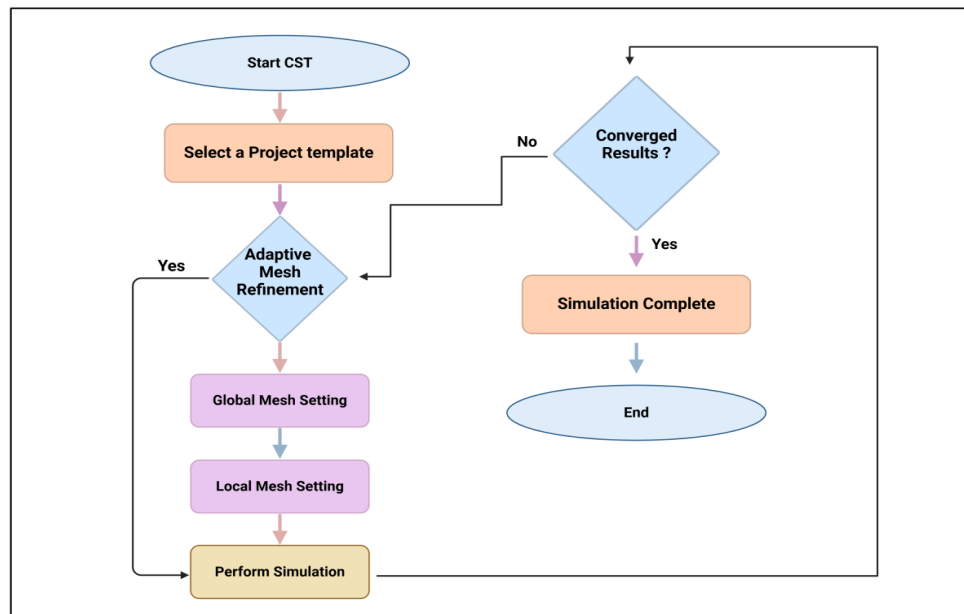


Figure 1. Algorithm of meshing flow in CST.

The Finite-Difference Time-Domain (FDTD) method calculates electromagnetic fields in CST by dividing Maxwell's equations in both spatial and temporal domains. Faraday's Law and Ampère's Law, both of which are partial differential equations, underpin the fundamental FDTD equations in CST. The central differences for the spatial and temporal derivatives are utilized to approximate these equations. Equation (1 and 2) represent the curl equations of Maxwell in a source-free zone.

$$\nabla \times \vec{E} = -\mu \frac{\partial \vec{H}}{\partial t} \tag{1}$$

$$\nabla \times \vec{H} = \epsilon \frac{\partial \vec{E}}{\partial t} \tag{2}$$

Where  $\vec{E}$ ,  $\vec{H}$  are the electric and magnetic field respectively,  $\mu$ ,  $\epsilon$  are the permeability and permittivity for a medium. The equations are analyzed in CST utilizing a uniform spatial grid with cell dimensions  $\Delta x$ ,  $\Delta y$ , and  $\Delta z$ , along with a minimal time increment  $\Delta t$  [24]. The FDTD approach entails sequential updating of the magnetic and electric fields at discrete time intervals. The fields are arranged in a staggered manner both spatially and temporally on a Yee grid. For clarity, below is a generalized representation of the update equations.

$$\vec{E}_x^{n+1}(i, j, k) = \vec{E}_x^n(i, j, k) + \frac{\Delta t}{\epsilon} \left( \frac{\vec{H}_z^{n+\frac{1}{2}}(i, j, k) - \vec{H}_z^{n+\frac{1}{2}}(i, j-1, k)}{\Delta y} - \frac{\vec{H}_y^{n+\frac{1}{2}}(i, j, k) - \vec{H}_y^{n+\frac{1}{2}}(i, j, k-1)}{\Delta z} \right) \tag{3}$$

$$\vec{H}_x^{n+1}(i, j, k) = \vec{H}_x^n(i, j, k) - \frac{\Delta t}{\mu} \left( \frac{\vec{E}_z^n(i, j, k+1) - \vec{E}_z^n(i, j, k)}{\Delta z} - \frac{\vec{E}_y^n(i, j+1, k) - \vec{E}_y^n(i, j, k)}{\Delta y} \right) \tag{4}$$

Where  $n$  is the current time step,  $(i, j, k)$  represent the grid values in the  $x, y,$  and  $z$  directions. The time step  $\Delta t$  is generally selected to comply with the Courant stability condition which given by equation (5) [24].

$$\Delta t \leq \frac{1}{c} \left[ \frac{1}{[1/\Delta x]^2 + [1/\Delta y]^2 + [1/\Delta z]^2} \right]^{\frac{1}{2}} \quad (5)$$

where  $c$  is the velocity of light. This criterion ensures the numerical solution stability. Finally, we can modify the boundary conditions. CST often uses Perfectly Matched Layer (PML) boundaries or other absorbing boundary conditions to reduce reflections at the edges of the simulation domain. This makes it easier to run an open-boundary simulation that more accurately simulates conditions in the real world. CST executes the FDTD equations on a spatial grid, iterating temporally to calculate the time-domain reaction of the electromagnetic fields across the structure.

### 3. Design Methodology

Optical Nano-antennas, which are usually about 100 nanometers long, are useful for optical purposes because they can create strong electromagnetic fields in areas smaller than a wavelength. Figure 2. illustrates the newly proposed design of the optical nanoantenna, known as the quadratic Koch fractal patch (QKF), and its complementary counterpart, the complementary quadratic Koch fractal patch (CQKF). The comprehensive perspective comprises three layers: ground, substrate, and patch. We fabricate the nano-antenna patch from gold metal. The patch dimensions are 500 nm in width ( $W_p$ ) and 500 nm in length ( $L_p$ ), with a thickness ( $t$ ) of 20 nm. The substrate layer, consisting of dielectric materials (silicon and silicon dioxide), has a thickness ( $h$ ) of 50 nm and dimensions of 900 nm by 900 nm. Gold, measuring 900 x 900 nm and with a thickness of 20 nm, forms the substrate. Table 1 delineates all parameters of the proposed nanoantenna.

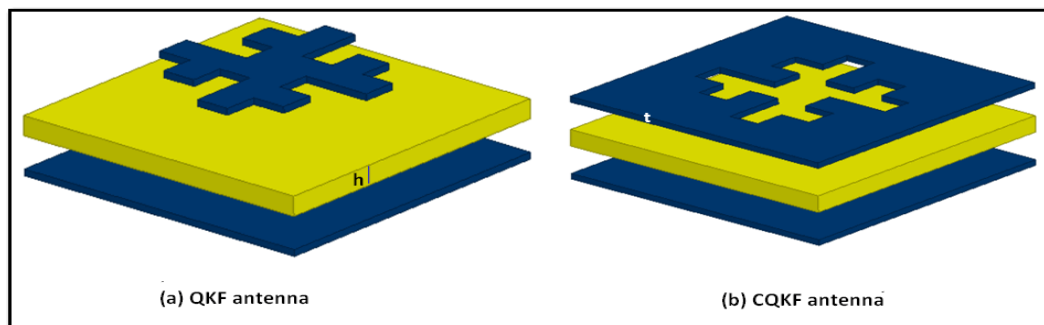


**Figure 2.** Nano-antenna design configuration.

The most direct method for generating high-performance fractals involves base and generator-type fractals. These are fractions created by iterative processes. The first steps to acquiring them involve selecting the segment, curve, or shape, and then the generator. We use an approach that repeats the same phase multiple times to create a new curve or shape from a previously established one, followed by iterative generation [25]. As its foundational shape, the proposed fractal antenna design is predicated on the geometry of a square patch. To create the fractal shape, apply a quadratic Koch fractal to each side of the square, as illustrated in Figure 3.

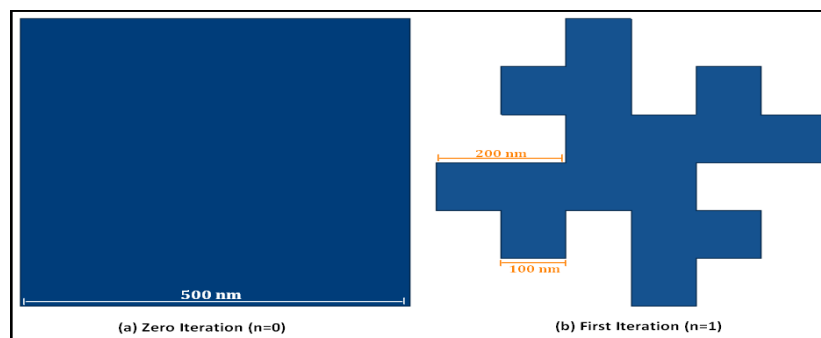


**Figure 3.** Fractal Patch Generation.

All four sides (segments) of a square shape replicate the Koch island generator. Each of those smaller segments represents a quarter of the original side of the substituted square. For planar fractal curves, a defining feature is their non-integer dimension, which varies between 1 and 2. The fractal's ability to occupy minute places is evaluated. The ratio in Eq. (6) yields the fractal dimensions of the Koch island, which is 1.5 [26].

$$D = \frac{\log(\text{Number of self similar segments})}{\log(\text{magnification factor})} \quad (6)$$

**Table 1:** Physical dimensions of the proposed Nanoantenna.

Nano antenna dimensions (nm)		
parameter	Discription	dimension
L	Substrate length	900
W	Substrate width	900
h	Thickness of Substrate	50
Lg	Ground length	900
Wg	Ground width	900
t	Ground & Patch Thickness	20
Lp	Patch length	500
Wp	Patch width	500

We construct the suggested nanoantenna on a silicon (Si) and silicon dioxide (SiO<sub>2</sub>) substrate, which have relative permittivity's of 11.9 and 4, respectively.

#### 4. Results and Discussion

We execute the design procedure using the Time Domain technique in CST Microwave Studio 2018. The performance assessment of QKF and CQKF for both substrate materials (Si and SiO<sub>2</sub>) reveals advantageous outcomes for gain and directivity. Directivity is an essential characteristic that measures the power density of an antenna's radiation in the direction of its peak power output. Figures 4 and 5 depict the three-dimensional gain and directivity of QKF and CQKF for silicon and silicon dioxide, respectively.

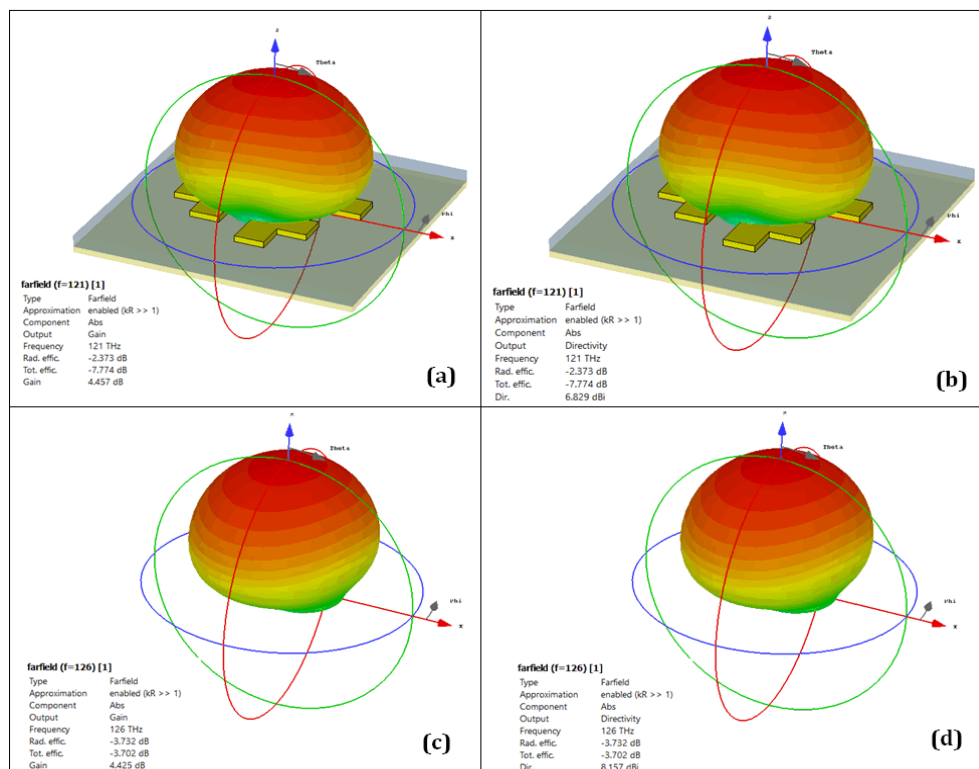


**Figure 4.** (a). Gain of QKF. (b). Directivity of QKF. (c). Gain of CQKF. (d). Directivity of CQKF.

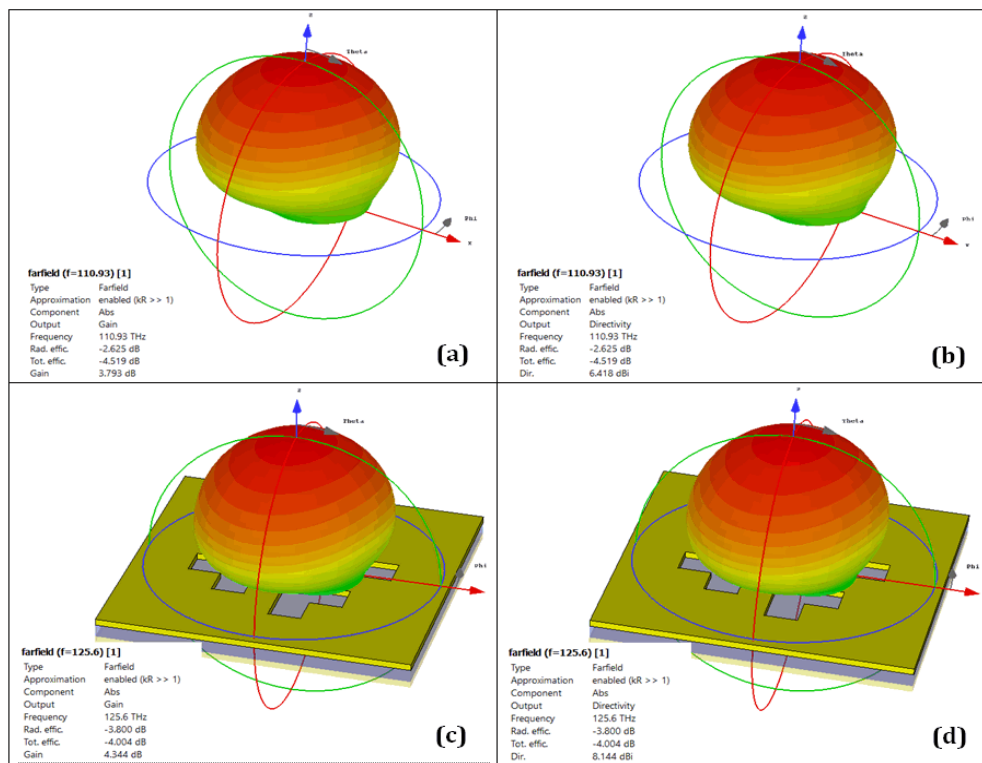


Figure 5. (a). Gain of QKF. (b). Directivity of QKF. (c). Gain of CQKF. (d). Directivity of CQKF.

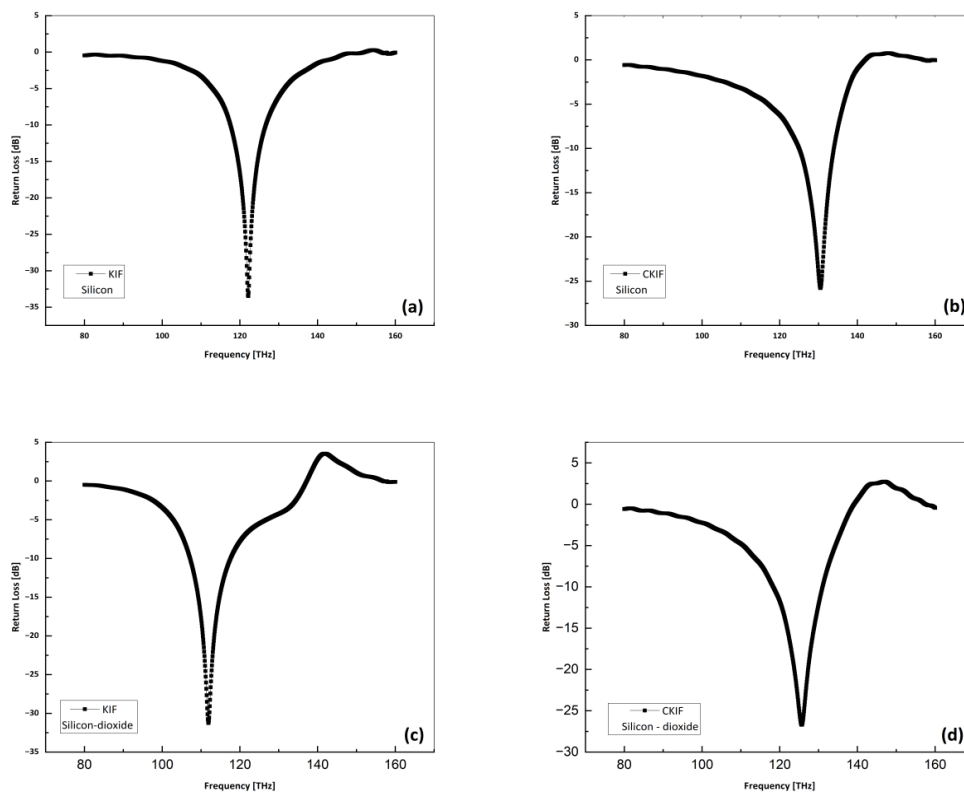


Figure 6. (a). S11 of QKF (Si). (b). S11 of CQKF (Si). (c). S11 of QKF (SiO2). (d). S11 of CQKF (SiO2).

Figure 6. shows the reflection coefficients (S11) for both QKF and CQKF nanoantennas as a function of frequency. It takes into account different substrate materials, such as silicon and silicon dioxide. In Figure 5a, the resonance frequency of the Quadratic Koch Fractal Nano Antenna (QKFNA) with a silicon dielectric substrate is 122.16 THz, with an S11 value of -33.47 dB and an operating bandwidth ranging from 117.6 THz to 126.56 THz. The complementary quadratic Koch fractal nanoantenna (CQKFNA) on a silicon substrate has a resonance frequency of 130 THz, an S11 of -25.7 dB, and a bandwidth that goes from 125.12 THz to 133.92 THz (Figure 5b). Figures 5c and 5d illustrate the S-parameters for both antennas utilizing a silicon dioxide (SiO2) substrate. Figure 5c illustrates that QKFNA's resonance frequency is 112 THz, with an S11 of -30.5 dB and a bandwidth ranging from 107.21 THz to 117.44 THz. Figure 5d shows that the resonant frequency for CQKFNA is 126 THz, with an S11 of -26 dB and a bandwidth ranging from 118.48 THz to 130.96 THz. Figure 7 illustrates the two-dimensional far-field patterns for both QKF and CQKF nanoantennas on a silicon substrate. Figure 8 illustrates the two-dimensional far-field patterns for both QKF and CQKF nanoantennas when silicon dioxide is used as a substrate.

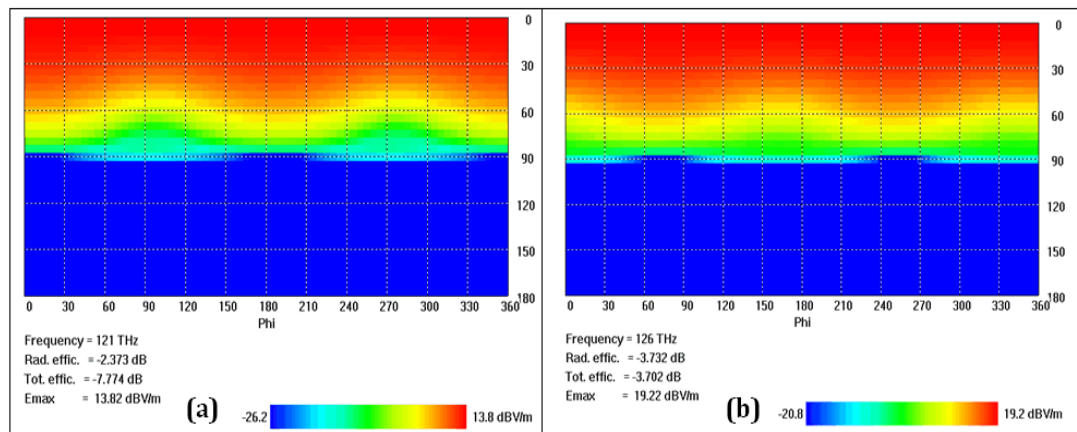


Figure 7. Shows the 2-dimensions farfield (a) QKF (b) CQKF.

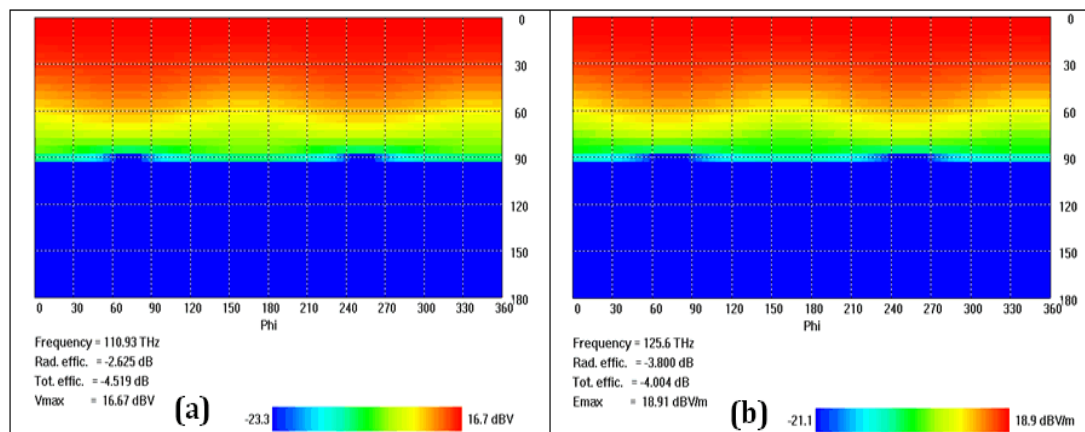


Figure 8. Shows the 2-dimensions farfield (a) QKF (b) CQKF.

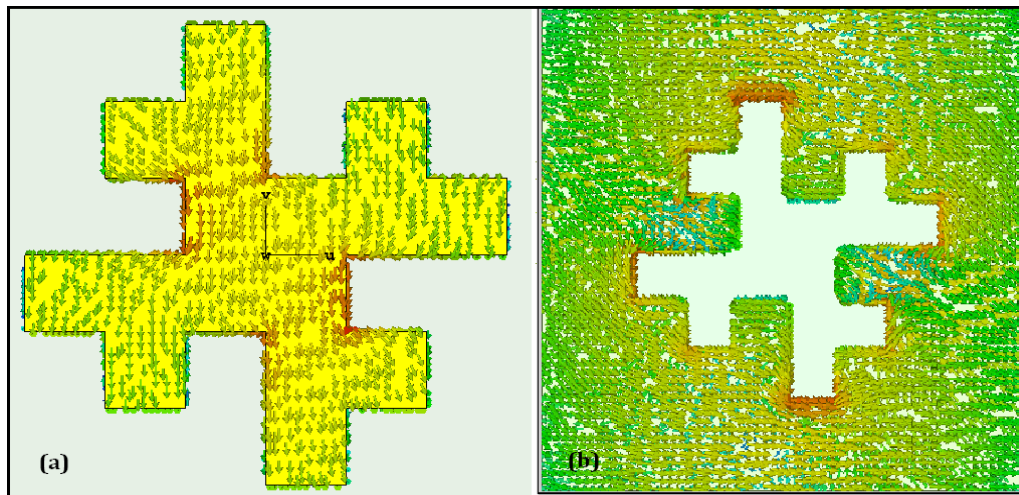
Table 2 presents the comprehensive results from QKFNA and CQKFNA (resonant frequency, bandwidth, return loss, gain, directivity, and antenna efficiency) as a function of relative permittivity. From equation (7), we can calculate the nanoantenna efficiency.

$$Eff. = \frac{Gain}{Directivity} \times 100\% \tag{7}$$

**Table 2:** The results obtained from QKFNA and CQKFNA

Substrate material	Antenna type	Resonant Frequency (THz)	Return loss (dB)	Gain (dB)	Directivity (dBi)	Bandwidth (THz)	Efficiency (Dimensionless)
Si ( $\epsilon_r=11.9$ )	QKFNA	122	-33.47	4.45	6.82	8.96	65%
	CQKFNA	130	-25.71	4.42	8.15	8.8	54%
SiO <sub>2</sub> ( $\epsilon_r=4$ )	QKFNA	112	-30.5	3.79	6.41	10.24	59%
	CQKFNA	126	-26	4.34	8.14	12.48	53%

The distribution of surface currents on the patch at resonant frequencies the two proposed nanoantennas are illustrated in Figure 9.

**Figure 9.** surface current distribution (a). (QKF). (b). (CQKF).

The various colors represented distinct magnitudes of current, as the resonant frequency for the proposed antenna operates in the terahertz region (high frequency). Consequently, the current follows more convoluted paths rather than straight ones, with the highest current values situated at the corners of the fractal patch, functioning like a U-slot. This phenomenon is referred to as the skin effect. As a result, at higher frequencies, current passes through the conductor's surface rather than its center portion.

## 5. Conclusion

We have designed and simulated the novel Quadratic Koch Fractal Nano-antenna (QKFNA) and its complimentary version, the Quadratic Koch Fractal Nano-antenna (CQKFNA), using CST Microwave Studio 2018. The two suggested nanoantennas on silicon substrate demonstrate differing resonant frequencies: 122.16 THz with a return loss of -33.47 dB for QKFNA and 130 THz with a return loss of -25.7 dB for CQKFNA. For silicon dioxide substrates, the resonance frequencies are 112 THz for QKFNA and 126 THz for CQKFNA, with both bands displaying a wide bandwidth ratio. Transitioning the fractal patch to a complementary configuration results in an increase in the resonance frequency from 122 to 130 THz. The silicon dioxide substrate experiences a frequency rise from 112 THz to 126 THz. Analyzing QKFNA's resonant frequencies in conjunction with two distinct substrate materials demonstrates a decrease in the resonant frequency from 122 to 112 THz. Similarly, when analyzing CQKFNA's resonant frequencies across two different substrate materials, we observe a reduction (antenna minimization) from 130 to 126 THz. Antenna efficiency is ascertained by the gain and directivity metrics. The arrangement of surface currents demonstrates that the fractal structure of the patch is crucial in regulating the surface current patch, hence affecting the antenna radiation pattern. The aforementioned designs employ a single waveguide port, enabling many applications like imaging spectroscopy, sensing, communication security surveillance, visible spectrum analysis, and mid-infrared (IR) detection.

**Funding:** "This research received no external funding"

**Conflicts of Interest:** "The authors declare no conflict of interest."

## References

- [1] Drégely D. Optical antennas: nanoscale radiation engineering and enhanced light-matter interaction 2014.
- [2] Biagioni P, Huang J-S, Hecht B. Nanoantennas for visible and infrared radiation. *Reports Prog Phys* 2012;75:24402. <https://doi.org/10.1088/0034-4885/75/2/024402>.
- [3] Hussein; Hussain RR. A WIDEBAND HYBRID PLASMONIC FRACTAL PATCH NANOANTENNA. *Int J Electron Commun Eng Technol* 2014;5:1–8.
- [4] Junk A, Riess F. From an idea to a vision: There’s plenty of room at the bottom. *Am J Phys* 2006;74:825–30. <https://doi.org/10.1119/1.2213634>.
- [5] Kavitha S, Mishra SK, Singh A, Singh SC.  $4 \times 4$  graphene nano-antenna array for plasmonic sensing applications. *Discov Appl Sci* 2024;6. <https://doi.org/10.1007/s42452-024-06161-0>.
- [6] Abbasi QH, Yang K, Chopra N, Jornet JM, Abuali NA, Qaraqe KA, et al. Nano-Communication for Biomedical Applications: A Review on the State-of-the-Art From Physical Layers to Novel Networking Concepts. *IEEE Access* 2016;4:3920–35. <https://doi.org/10.1109/access.2016.2593582>.
- [7] Cheerla S, Subbareddy V, Sudha Harika T, Yalla J, Pamulapati P. Design and Analysis of Plasmonic Antenna for Nanoscale Wireless Applications. *J Phys Conf Ser* 2021;1804:12164. <https://doi.org/10.1088/1742-6596/1804/1/012164>.
- [8] Elsaid M, Mahmoud KR, Hussein M, Hameed MFO, Obayya SSA. Improvement of sectoral horn nanoantenna based on arc directors for point to point communications. *Opt Quantum Electron* 2021;53. <https://doi.org/10.1007/s11082-021-02788-0>.
- [9] Zhao Y, Alu A. Optical nanoantennas and their applications. 2013 IEEE Radio Wirel Symp 2013:58–60. <https://doi.org/10.1109/rws.2013.6486640>.
- [10] Alù A, Engheta N. Wireless at the Nanoscale: Optical Interconnects using Matched Nanoantennas. *Phys Rev Lett* 2010;104. <https://doi.org/10.1103/physrevlett.104.213902>.
- [11] Novotny L. Effective Wavelength Scaling for Optical Antennas. *Phys Rev Lett* 2007;98. <https://doi.org/10.1103/physrevlett.98.266802>.
- [12] Pfeiffer C. Fundamental Efficiency Limits for Small Metallic Antennas. *IEEE Trans Antennas Propag* 2017;65:1642–50. <https://doi.org/10.1109/tap.2017.2670532>.
- [13] Shenker OR. Fractal geometry is not the geometry of nature. *Stud Hist Philos Sci Part A* 1994;25:967–81. [https://doi.org/10.1016/0039-3681\(94\)90072-8](https://doi.org/10.1016/0039-3681(94)90072-8).
- [14] Sidhu AK, Sivia JS. Design of Wideband Fractal MIMO Antenna using Minkowski and Koch Hybrid Curves on Half Octagonal Radiating Patch with High Isolation and Gain for 5G Applications. *Adv Electromagn* 2023;12:58–69. <https://doi.org/10.7716/aem.v12i1.1982>.
- [15] Gianvittorio JP, Rahmat-Samii Y. Fractal antennas: a novel antenna miniaturization technique, and applications. *IEEE Antennas Propag Mag* 2002;44:20–36. <https://doi.org/10.1109/74.997888>.
- [16] Anguera J, Andújar A, Jayasinghe J, Chakravarthy VVSSS, Chowdary PSR, Pijoan JL, et al. Fractal Antennas: An Historical Perspective. *Fractal Fract* 2020;4:3. <https://doi.org/10.3390/fractalfract4010003>.
- [17] Sanu SV, Rodrigues S, Vallikkunel JKN, Sivan SA. Fractal-Enhanced Microstrip Antennas: Miniaturization, Multiband Performance and Cross-Polarization Minimization for Wi-Fi Applications. *RAiSE-2023* 2023:127. <https://doi.org/10.3390/engproc2023059127>.
- [18] Froumsia D, Jean-François ED, Houwe A, Kolyang, Inc M. Miniaturization of dual bands fractal-based microstrip patch fractal antenna for X and Ku bands applications. *Eur Phys J Plus* 2022;137. <https://doi.org/10.1140/epjp/s13360-022-02969-0>.
- [19] Wang L, Yu J, Xie T, Bi K. A Novel Multiband Fractal Antenna for Wireless Application. *Int J Antennas Propag* 2021;2021:1–9. <https://doi.org/10.1155/2021/9926753>.
- [20] Attioui S, El Ouadi Z, El Aoud SE, Ibnyaich S, Zeroual A. Design of Multiband Fractal Antenna Array for Wireless Communication. *ITM Web Conf* 2023;52:3006. <https://doi.org/10.1051/itmconf/20235203006>.
- [21] Karlina S, Nugroho BS, Citra Atmaja AH, Ismail N. Ultra-Wideband Antenna for Bandwidth Enhancement Telkomsel Orbit Mobile Wifi. 2023 9th Int Conf Wirel Telemat 2023:1–5. <https://doi.org/10.1109/icwt58823.2023.10335417>.
- [22] Komeylian S, Paolini C. Performance Evaluation of a Fractal Plasmonic Bowtie Nano-Antenna: Optical and Far-Field Properties. *IEEE Trans Nanotechnol* 2024;23:9–19. <https://doi.org/10.1109/tnano.2023.3332555>.
- [23] Pahuja A, Kumar S, Parihar MS, Dinesh Kumar V. Half Euler Spiral Nanoantenna based Smart City Compatible Thin Film Solar Cell. 2023 IEEE 7th Conf Inf Commun Technol 2023:1–4. <https://doi.org/10.1109/cict59886.2023.10455675>.

- [24] Sullivan, Dennis M. Electromagnetic simulation using the FDTD method. John Wiley & Sons, 2013.
- [25] Paun M, Nichita M, Paun V, Paun V. Fifth-generation fractal antenna design based on the <scp>Koch Snowflake geometry. A fractal theory application. Expert Syst 2023. <https://doi.org/10.1111/exsy.13242>.
- [26] Nurujjaman M. A Review of Fractals Properties: Mathematical Approach. Sci J Appl Math Stat 2017;5:98. <https://doi.org/10.11648/j.sjams.20170503.11>.